

Minimum detectable damage for stochastic subspace-based methods

Alexander Mendler, Saeid Allahdadian, Michael Dohler, Laurent Mevel, Carlos Ventura

▶ **To cite this version:**

Alexander Mendler, Saeid Allahdadian, Michael Dohler, Laurent Mevel, Carlos Ventura. Minimum detectable damage for stochastic subspace-based methods. IOMAC 2019 - 8th International Operational Modal Analysis Conference, May 2019, Copenhague, Denmark. pp.1-11. hal-02142994

HAL Id: hal-02142994
https://inria.hal.science/hal-02142994

Submitted on 29 May 2019

HAL is a multi-disciplinary open access archive for the deposit and dissemination of scientific research documents, whether they are published or not. The documents may come from teaching and research institutions in France or abroad, or from public or private research centers.

L'archive ouverte pluridisciplinaire **HAL**, est destinée au dépôt et à la diffusion de documents scientifiques de niveau recherche, publiés ou non, émanant des établissements d'enseignement et de recherche français ou étrangers, des laboratoires publics ou privés.

IOMAC'19
8th International Operational Modal Analysis Conference
2019 May12-14 Copenhagen

MINIMUM DETECTABLE DAMAGE FOR STOCHASTIC SUBSPACE-BASED METHODS

A. Mendler[1], *S. Allahdadian*[2], *M. Döhler*[3] , *L. Mevel*[4], *C.E. Ventura*[5]

[1] Ph.D. Candidate, University of British Columbia, Department of Civil Engineering, Canada, alexander.mendler@ubc.ca.
[2] Researcher, University of British Columbia, Department of Civil Engineering, Canada, saeid@civil.ubc.ca.
[3] Researcher, Inria, Ifsttar, I4S, Rennes, France, michael.doehler@inria.fr.
[4] Senior researcher, Inria, Ifsttar, I4S, Rennes, France, laurent.mevel@inria.fr
[5] Professor, University of British Columbia, Department of Civil Engineering, Canada, ventura@civil.ubc.ca.

ABSTRACT
Detecting small and local damages on structures based on ambient vibrations is a major challenge in structural health monitoring. However, being able to identify the minimum damage is essential for quantifying the effectiveness of the instrumentation and for defining the limitations of low-frequency vibration monitoring in general. This paper shows how subspace-based methods could be used by engineers to predict the minimum damage that can be detected. The method employs a Gaussian subspace-based residual vector as a damage-sensitive criterion and evaluates its deviation from zero mean through two different statistical hypothesis tests, a parametric version and a non-parametric one. A sensitivity analysis is carried out to parametrize the deviation from the nominal state, and link it to physical parameters in a finite element model through the Fisher information matrix. This link can also be used to predict the minimum detectable damage, *e.g.* by prescribing a minimum probability of detection based on code-based reliability concepts. Ultimately, the developed theory is verified by means of a numerical example.

Keywords: Ambient vibrations, statistical hypothesis test, Fisher information, finite element model

1. INTRODUCTION

In the literature, many techniques have been proposed to monitor the health state of structures based on ambient vibrations [1]. Moreover, there seems to be a general consent that output-only methods based on ambient vibrations may not be sensitive enough to diagnose small and local damages, due to the low damage-related information content of low-level or low-frequency vibrations. Therefore, it has become a key issue to quantify the minimum detectable damage that vibration-based methods can sense based on the global system response (for instance in percent of a stiffness parameter), because it allows to explicitly assess the efficiency of a monitoring system, and helps to transition state-of-the-art technology into engineering practice [2].

Stochastic subspace-based methods offer means to quantify the minimum detectable damage, because the healthy and the damaged state can be linked through a statistical framework using the Fisher information matrix. The foundations were laid in 1987 by introducing the underlying statistical expressions, also called the asymptotic local approach [3]. In 2000, the first attempt to use subspace-based methods for damage detection was documented [4]. In essence, a subspace-based residual is computed with zero mean in the reference state and non-zero mean in the damaged state. To give physical meaning to the statistical criterion, it was linked to mechanical parameters in a finite element (FE) model that would experience changes due to damage in the real structure. This was, for example, done by means of a sensitivity analysis of the residual toward the affected parameters [5]. An improved residual was published in 2014 that was more robust toward variations in the ambient excitation characteristics [6]. In this paper, a predictive formula is developed that takes as input the vibration data of a healthy structure and the parameters of a corresponding FE model, and predicts the minimum damage by requiring a minimum damage resolution for decision making. The derivation is shown for two damage diagnosis tests, the parametric and non-parametric detection test, and validated by means of a numerical example.

2. BACKGROUND

2.1. Stochastic Subspace

This first section recaps how the stochastic subspace can be estimated from ambient vibrations. The starting point is a discrete state space model used to describe a linear and time-invariant mechanical system with m degrees of freedom (DOF) under random excitation:

$$\begin{cases} \mathbf{x}_{k+1} &= \mathbf{A}\mathbf{x}_k + \mathbf{w}_k \\ \mathbf{y}_k &= \mathbf{C}\mathbf{x}_k + \mathbf{v}_k, \end{cases} \tag{1}$$

where $\mathbf{A} \in \mathbb{R}^{n\times n}$ and $\mathbf{C} \in \mathbb{R}^{r\times n}$ are the state transition and the output matrix and $n = 2m$. The vectors $\mathbf{x}_k \in \mathbb{R}^{n\times 1}$ and $\mathbf{y}_k \in \mathbb{R}^{r\times 1}$ are the state vector and the measurement vector at time instant k, and $\mathbf{w}_k \in \mathbb{R}^{n\times 1}$ and $\mathbf{v}_k \in \mathbb{R}^{r\times 1}$ are noise terms modeled as white noise. First, the output covariances $\mathbf{R}_i = \mathbf{E}(\mathbf{y}_{k+i}\mathbf{y}_k)$ are estimated and assembled in the block Hankel matrix

$$\boldsymbol{\mathcal{H}}_{p+1,q} = \begin{bmatrix} \mathbf{R}_1 & \mathbf{R}_2 & \dots & \mathbf{R}_q \\ \mathbf{R}_2 & \mathbf{R}_3 & \dots & \mathbf{R}_{q+1} \\ \vdots & \vdots & \ddots & \vdots \\ \mathbf{R}_{p+1} & \mathbf{R}_{p+2} & \dots & \mathbf{R}_{p+q} \end{bmatrix}; \qquad \mathbf{R}_i = \mathbf{R}_{yy,i} = \frac{1}{N-i}\sum_{k=1}^{N-i} \mathbf{y}_{k+i}\mathbf{y}_k^T. \tag{2}$$

The time lags $i = 1, \dots, p+q$ are used to evaluate the similarity of the time-shifted wave patterns at different sensor locations, where p and q should be chosen sufficiently large with $\min(pr, qr) \geq n$ and often $p + 1 = q$. Secondly, the matrix is decomposed into its subspaces by means of a singular value decomposition separating the orthonormal singular vectors related to structural information $\mathbf{U}_1$ from those related to noise processes $\mathbf{U}_0$, also referred to as the left null-space.

$$\boldsymbol{\mathcal{H}}_{p+1,q} = \begin{bmatrix} \mathbf{U}_1 & \mathbf{U}_0 \end{bmatrix} \begin{bmatrix} \mathbf{D}_1 & \mathbf{0} \\ \mathbf{0} & \mathbf{D}_0 \end{bmatrix} \begin{bmatrix} \mathbf{V}_1^T \\ \mathbf{V}_0^T \end{bmatrix} \tag{3}$$

2.2. Damage Diagnosis

A damage-sensitive criterion is formed by multiplying the left null-space from the training phase with the block Hankel matrix estimated from test data. When vectorized by means of the column stacking operator $vec(\cdot)$ and scaled by the square root of the sample size, it is also called the Gaussian residual.

$$\boldsymbol{\zeta} = \sqrt{N} vec(\mathbf{U}_0^T \boldsymbol{\mathcal{H}}_{p+1,q}) \sim \begin{cases} \mathcal{N}(\mathbf{0}, \boldsymbol{\Sigma}) & healthy \\ \mathcal{N}(\boldsymbol{\mathcal{J}}\boldsymbol{\delta}, \boldsymbol{\Sigma}) & damaged, \end{cases} \tag{4}$$

where the covariance $\boldsymbol{\Sigma}$ is estimated as the sample covariance from realizations $\boldsymbol{\zeta}_k$ of the residual computed on blocks of the available data [6] with

$$\boldsymbol{\Sigma} = \frac{1}{n_b - 1} \sum_{k=1}^{n_b} \boldsymbol{\zeta}_k \boldsymbol{\zeta}_k^T. \tag{5}$$

If no damage is present, the residual follows a normal distribution with zero mean and covariance $\boldsymbol{\Sigma}$. Any abnormality in the test data causes a deviation from zero mean that can be parametrized as $\boldsymbol{\mathcal{J}}\boldsymbol{\delta}$, that is, the sensitivity of the Gaussian residual toward changes in any structural parameters $\boldsymbol{\mathcal{J}} = \partial \mathbf{E}(\frac{1}{\sqrt{N}}\boldsymbol{\zeta})/\partial \boldsymbol{\theta}$ multiplied by the parameter change vector $\boldsymbol{\delta} = \sqrt{N}(\boldsymbol{\theta} - \boldsymbol{\theta}_0)$. To assess the significance of the deviation, the general likelihood ratio can be employed. It quantifies the likelihood that the residual is drawn from the probability distribution corresponding to the damaged structure rather than the healthy one. Using the matrices from above, the likelihood ratio can be expressed as [6]

$$t = \boldsymbol{\zeta}^T \boldsymbol{\Sigma}^{-1} \boldsymbol{\mathcal{J}} \left(\boldsymbol{\mathcal{J}}^{\boldsymbol{T}} \boldsymbol{\Sigma}^{\boldsymbol{-1}} \boldsymbol{\mathcal{J}} \right)^{\boldsymbol{-1}} \boldsymbol{\mathcal{J}}^T \boldsymbol{\Sigma}^{-1} \boldsymbol{\zeta} \sim \begin{cases} \chi^2(k, 0) & healthy \\ \chi^2(k, \lambda) & damaged \end{cases}. \tag{6}$$

The test statistic t is scattered due to the stochastic nature of the method. As shown in [7], it follows a chi-squared distribution with k degrees of freedom and a non-centrality of zero $\lambda = 0$ in the healthy state. In the damaged state, the non-centrality is $\lambda = \boldsymbol{\delta}^T (\boldsymbol{\mathcal{J}}^T \boldsymbol{\Sigma}^{-1} \boldsymbol{\mathcal{J}}) \boldsymbol{\delta}$, and serves as a measure for the severity of damage, see Fig. 1. If no parametrization is available, the sensitivity of the parametrization toward the residual vector defaults to unity $\boldsymbol{\mathcal{J}} = \mathbf{I}$, and the general likelihood ratio from Eq. (6) collapses into

$$t = \boldsymbol{\zeta}^T \boldsymbol{\Sigma}^{-1} \boldsymbol{\zeta} \sim \begin{cases} \chi^2(k, 0) & healthy \\ \chi^2(k, \lambda) & damaged \end{cases}. \tag{7}$$

To decide whether the structure is damaged or not, the test statistic from Eq. (6) or (7) is compared against a threshold t_{crit}, and an alarm is sound if $t > t_{crit}$.

2.3. Parametrization

Damage can be parametrized, meaning the deviation in the mean residual from Eq. (4) can be linked to the structural parameter that caused it. To do that, two *modal* parameter vectors have to be established, storing all poles and mode shapes that characterize the vibration behaviour in discrete-time and continuous-time. Moreover, a *physical* parameter vector $\boldsymbol{\theta}$ is defined, which holds structural parameters that may experience changes. For a mass-and-spring system with one DOF, a full parametrization writes

$$\boldsymbol{\theta}_d = \begin{bmatrix} Re(\lambda) \\ Im(\lambda) \\ vec(Re(\phi)) \\ vec(Im(\phi)) \end{bmatrix}, \boldsymbol{\theta}_c = \begin{bmatrix} Re(\mu) \\ Im(\mu) \\ vec(Re(\phi)) \\ vec(Im(\phi)) \end{bmatrix}, \boldsymbol{\theta} = \begin{bmatrix} m \\ c \\ k \end{bmatrix}. \tag{8}$$

Linking the mean residual to a change in the parameter vector $\boldsymbol{\theta}$ is done by means of three consecutively performed first-order sensitivity analyses [8]. The first Jacobian matrix holds the sensitivity of the mean residual toward the discrete poles and mode shapes evaluated based on operational modal analysis concepts [4, 6, 9]. The second Jacobian matrix links the modal parameters to the ones of the analytical model, which are in continuous-time [9]. The third Jacobian matrix links the analytical modal parameters to the structural parameters [5], *e.g.* by means of the direct sensitivity approach [10].

$$\boldsymbol{\mathcal{J}} = \frac{\partial}{\partial \boldsymbol{\theta}} \mathbf{E}(\tfrac{1}{\sqrt{N}}\boldsymbol{\zeta}) = \boldsymbol{\mathcal{J}}_{\boldsymbol{\theta}_d}^{\boldsymbol{\zeta}} \boldsymbol{\mathcal{J}}_{\boldsymbol{\theta}_c}^{\boldsymbol{\theta}_d} \boldsymbol{\mathcal{J}}_{\boldsymbol{\theta}}^{\boldsymbol{\theta}_c} \tag{9}$$

If the modal parameter vectors are incomplete, modal truncation occurs and biases the damage diagnosis. However, the physical parameter vector can be defined by the user, meaning a reduced set of monitoring parameter can be chosen, and no bias is introduced if damage only affects the selected parameters.

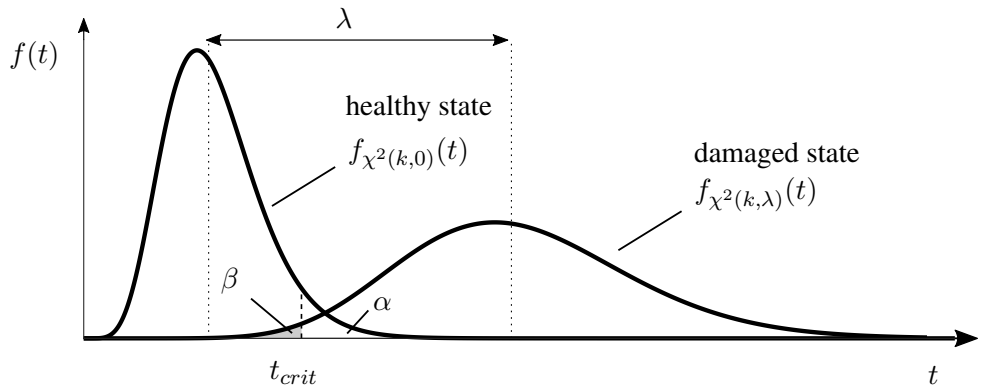


Figure 1: Statistical distribution of the test statistic for damage detection.

3. LINKING HEALTHY AND DAMAGED STATE

3.1. Parametric Detection Test

As mentioned above, different structural health states can be linked through the non-centrality parameter, which changes from $\lambda = 0$ in the healthy state to $\lambda = \boldsymbol{\delta}^T(\boldsymbol{\mathcal{J}}^T\boldsymbol{\Sigma}^{-1}\boldsymbol{\mathcal{J}})\boldsymbol{\delta}$ in the damaged one. On close inspection, it becomes clear that the bracket term can be calculated based on healthy vibration data, so all information on the future shift in the test statistic due to damage is already available. It corresponds to the information matrix or the Fisher information matrix of the parameter $\boldsymbol{\theta}$ contained in the residual $\boldsymbol{\zeta}$.

$$\mathbf{F} = \boldsymbol{\mathcal{J}}^T\boldsymbol{\Sigma}^{-1}\boldsymbol{\mathcal{J}} \tag{10}$$

As explained in Section 2.3., all physical parameters to be monitored are user-defined, and the only requirement is that structural changes only occur in the physical parameters that are stored in $\boldsymbol{\theta}$. In the special case, where damage is limited to a single parameter θ_i in $\boldsymbol{\theta}$, the shift of the mean value from zero is only due to the damage in that very parameter $\boldsymbol{\mathcal{J}}\boldsymbol{\delta} = \boldsymbol{\mathcal{J}}_i\delta_i$, where $\boldsymbol{\mathcal{J}}_i$ is the ith column of the sensitivity matrix. For this case, the Fisher information reduces to a scalar value, and the relation between the healthy and damaged state writes

$$\lambda = F_{ii}\delta_i^2. \tag{11}$$

That means that the non-centrality parameter λ from the statistical test can be linked to a physical parameter change of a single structural parameter δ_i in an analytical computer model through the main diagonal value of the Fisher information, making F_{ii} a measure for the detectability of damage [11].

3.2. Non-parametric Detection Test

In the non-parametric test from Eq. (7), the test statistic t is evaluated without taking into account the sensitivity matrix $\boldsymbol{\mathcal{J}}$, but this section explains why the healthy and damaged state can still be linked through the Fisher information according to Eq. (10) and (11). For this purpose, a new vector $\mathbf{z}$ with unit variance is defined by pre-multiplying $\boldsymbol{\Sigma}^{-1/2}$ to the residual of the damaged state from Eq. (4).

$$\mathbf{z} = \boldsymbol{\Sigma}^{-1/2}\boldsymbol{\zeta} \sim \mathcal{N}(\boldsymbol{\Sigma}^{-1/2} \cdot \boldsymbol{\mathcal{J}}\boldsymbol{\delta}, \mathbf{I})$$

Squaring up this vector yields the non-parametric test statistic

$$t = \mathbf{z}^T\mathbf{z} = \boldsymbol{\zeta}^T\boldsymbol{\Sigma}^{-1}\boldsymbol{\zeta} \sim \chi^2(k, \lambda), \tag{12}$$

with the non-centrality parameter

$$\lambda = \boldsymbol{\mu}^T\boldsymbol{\mu} = (\boldsymbol{\Sigma}^{-1/2}\boldsymbol{\mathcal{J}}\boldsymbol{\delta})^T(\boldsymbol{\Sigma}^{-1/2}\boldsymbol{\mathcal{J}}\boldsymbol{\delta}) = \boldsymbol{\delta}^T(\boldsymbol{\mathcal{J}}^T\boldsymbol{\Sigma}^{-1}\boldsymbol{\mathcal{J}})\boldsymbol{\delta}. \tag{13}$$

3.3. Practical Considerations

This section presents an approach to interpret the non-centrality λ from an engineering perspective. Obviously, λ quantifies the degree of separation between the distributions related to the healthy and damaged state (see Fig. 1), so it can be interpreted as some kind of reliability index. The larger the non-centrality, the lower the probability that the structure is mistakenly diagnosed as healthy although it is not, and vice versa. However, there will always be an overlap between the two states. The following paragraphs give guidance on how to choose an appropriate λ for a specific monitoring application by tying it back to code-based reliability concepts.

3.3.1. Reliability Concept

The first question one should ask oneself is "how often do I want the test to diagnose the structure as damaged although it is not"? Based on the accepted false-negative rate (type I error α), a safety threshold value can be defined for the test statistic, see t_{crit} in Fig. 1. For civil engineering structures, a typical type I error could be in the range of $\alpha = [0.3\%, 5\%]$ or lower, meaning one out of 20 - 300 tests diagnoses a healthy structure as damaged.

The second question is "how often do I want the test to diagnose the structure as undamaged although damage is present"? The false-positive rate (type II error β) is critical and depends on the allowable damage consequences. For load-bearing components, for example, it is recommended to choose the type II error according to the national reliability concept. In Canada and the U.S.A., the reliability index for assessment is defined as 3.25 and 2.5, which is equivalent to a false-negative rate of $\beta = 0.06\%$ and $\beta = 0.6\%$, respectively. The Eurocode does not define a reliability index for assessment, but the ISO norm requires a reliability index of 4.7, so $\beta = 10^{-6}$ [12].

3.3.2. Corresponding Non-centrality

Once the type I and II errors are defined, the non-centrality parameter λ can be solved for as the distance between the mean values of the healthy and damaged state PDF. There is still one unknown, that is the number of degrees of freedom k, but since this value depends on the kind of damage diagnosis test that is performed (*e.g.* parametric, or non-parametric detection test, or others), it is treated as a known constant here and referred to Section 3.3.3. below. Graphically, the defined type I error α describes the area under the healthy state PDF to the right of the safety threshold t_{crit}, see Fig. 1. When setting up the corresponding equation, the only unknown is t_{crit}, which can be solved for, *e.g.* by means of the cumulative distribution function (CDF) for the healthy state $F_{\chi^2(k,0)}(t_{crit})$ and numerical iteration.

$$\alpha = 1 - \int_0^{t_{crit}} f_{\chi^2(k,0)}(t)dt = 1 - F_{\chi^2(k,0)}(t_{crit}) \tag{14}$$

The type II error β corresponds to the area below the damaged state PDF to the left of the safety threshold. The only unknown in the following equation is the desired non-centrality λ, which can be solved for in the same manner as for the safety threshold using the CDF of the damaged state $F_{\chi^2(k,\lambda)}(t_{crit})$.

$$\beta = \int_0^{t_{crit}} f_{\chi^2(k,\lambda)}(t)dt = F_{\chi^2(k,\lambda)}(t_{crit}) \tag{15}$$

3.3.3. Number of Degrees of Freedom

The number of degrees of freedom k of the chi-squared distribution can be interpreted as a measure for the dimensionality of the damage detection problem, so it depends on the specific monitoring application. Mathematically, k corresponds to the number of statistical processes that influence the dynamic behaviour of the structure. In some special cases, k coincides with the number of parameters to be monitored. Suppose, all contributing factors are collected in a parameter vector $\boldsymbol{\theta}$ in Eq. (8). Further suppose that the individual parameters θ_i do not influence each other and their effect on the residual can be clearly

distinguished; then, the sensitivity matrix $\mathcal{J}$ has full rank, and k corresponds to the number of columns in the sensitivity matrix, which is equal to the number of parameters in $\boldsymbol{\theta}$. For the non-parametric test, k is equal to the rank of the (converged) covariance matrix. However, this theoretical criterion is not very meaningful for practical applications, because the singular values of the covariance estimate decrease continuously without showing a distinct jump.

Alternatively, auxiliary empirical tools can be used to estimate k. For example, the statistical distribution from Eq. (6) and (7) for the healthy state could be evaluated in a Monte Carlo simulation. Then, it could be subdivided into bins, and a least-square fit could be performed with k being the only variable in the target function of a central chi-square distribution ($\lambda = 0$).

$$f_{\chi^2(k,0)}(t) = \frac{1}{2^{k/2}\Gamma(k/2)} t^{k/2-1} e^{-t/2}. \tag{16}$$

3.4. Predictive Formula

By bringing together the considerations from previous sections, a predictive formula can be developed for the minimum detectable damage. The starting point is a fundamental statistical equation, the asymptotic local approach. It describes the relation between the parameter change vector $\boldsymbol{\delta}$ and the chosen parametrization and includes a scaling factor for the measurement duration, which guarantees that the residual follows a normal distribution and that the log-likelihood of the general likelihood test is well-defined. [3]

$$(\boldsymbol{\theta} - \boldsymbol{\theta}_0) = \boldsymbol{\delta}/\sqrt{N}$$

A predictive formula for the minimum detectable damage in each individual parameter i is obtained by substituting $N = T f_s$ as well as the relation $\lambda = \delta_i^2 F_{ii}$ from Eq. (11). When normalized by the reference parameter vector, the parameter change is given in percent and can be associated with a measure for the damage severity $\Delta_i = (\theta_i - \theta_{0,i})/\theta_{0,i}$.

$$\Delta_i = \frac{1}{\theta_{0,i}} \sqrt{\frac{\lambda}{T f_s \cdot F_{ii}}} [\%] \tag{17}$$

This formula for the minimum detectable damage Δ_i includes three variables, namely the measurement duration and sampling frequency, T and f_s, and the non-centrality parameter λ, which is a function of the accepted type I and II errors α and β and the number of degrees of freedom k. The relative magnitude of the monitoring parameter $\theta_{0,i}$, on the other hand, depends on the structural system, and the Fisher information F_{ii} depends on the sensor configuration as well as T, f_s and $\theta_{0,i}$.

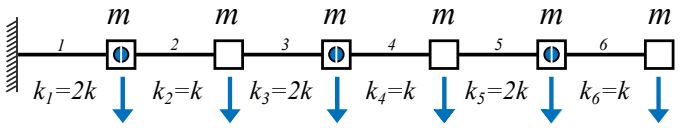


Figure 2: 6-DOF mass-and-spring system instrumented with three sensors (round symbols).

4. APPLICATION

For validation, the methodology was applied to a 6-DOF mass-and-spring system with a fundamental frequency of 2.03 Hz (T = 0.49 s). Lumped masses of 1.0 t were connected through beams with alternating stiffness values, where k = 2000 MN/m (see Fig. 2). Rotational DOFs were fixed and gravity effects were neglected. Every mode of vibration was assumed to be lightly damped with a modal damping ratio of 2% critical damping. A white noise excitation was generated and applied along all DOFs. Three sensors were placed at the masses 1, 3, 5 sampling the signal at 128 Hz. The type I and II errors were set to $\alpha = \beta = 2\%$ for demonstration purposes. For clarity, the following sections are organized in the three main states of the damage diagnosis: the reference state, the training state and the test state.

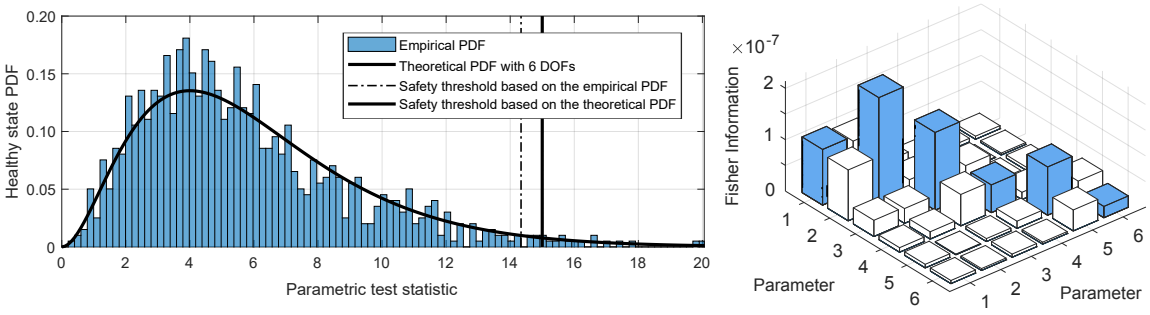


Figure 3: Healthy state PDF of the parametric test (left), and Fisher information matrix (right).

4.1. Reference State

In the reference state, all matrices were determined for the damage diagnosis test and for the prediction of the minimum detectable damage. Firstly, the parametrization was defined, and to avoid modal truncation, all six modes of vibration were considered. A common engineering assumption is to only consider a stiffness decrease due to damage, so the parameter vector from Eq. (8) reduced to

$$\boldsymbol{\theta}_0 = [k_1, k_2, k_3, k_4.k_5, k_6]^T. \tag{18}$$

Secondly, the residual vector from Eq. (4) was evaluated based on vibration data of the healthy structure, and both its covariance $\boldsymbol{\Sigma}(\boldsymbol{\zeta})$ and sensitivity toward the parameter vector from Eq. (18) were calculated according to Eq. (5) and (9). Moreover, the Fisher information matrix was computed based on Eq. (10) and visualized as shown in Fig 3. In this example, the measurement duration was set to a large value of $T_0 = 300$ min to reduce the uncertainties in the Gaussian residual and all matrices derived from it.

4.2. Training State

In the training state, the healthy state PDF from Fig. 1 was determined with the only unknown being the number of degrees of freedom k. For the non-parametric test, no theoretical value was available for k, so it had to be determined empirically. To do so, 1,000 ambient vibration records with a measurement duration of $T = 1$ min were created in a Monte Carlo experiment while applying the damage diagnosis test from Eq. (7) to each record. Then, the empirical distribution was plotted in a histogram and the curve from Eq. (16) was fitted. A minimum error was achieved for $k = 82$, a value that was higher than the number of parameters to be monitored but lower than the number of rows/columns in the covariance matrix (160). That means the covariance matrix was not of full rank.
For the parametric test, the number of degrees of freedom was set to the theoretical value of $k = 6$, as six parameters were to be monitored, see Eq. (18), but its distribution was evaluated as well for comparison, see Fig. 3. The empirical distribution (in bright blue) appeared to follow the theoretical one (solid black line), so the assumption of a full rank sensitivity matrix was justified. Moreover, the curve fitting approach could be validated, as it resulted in the same value for the number of degrees of freedom.

The healthy state was now fully defined, because the non-centrality parameter was assumed to be zero $\lambda = 0$, and the safety threshold t_{crit} could be determined as the quantile value of the chi-square distribution corresponding to the predefined type I error $Q[f_{\chi^2(k,0)}(t)] = \alpha$. This approach was convenient and efficient because an empirical evaluation in the training state is circumvented for the parametric test.

4.3. Predicting the Minimum Damage

Having completed the training phase, the minimum detectable damage could be predicted according to Eq. (17) with the only remaining unknown being the (minimum) non-centrality parameter λ. It could be determined as the distance between the mean values of the healthy and damaged state, see Fig. 1, taking as input the accepted type I and II error, α and β, as well as the number of degrees of freedom k of the healthy state PDF, see Eq. (14) and (15).

4.4. Test State

In the test phase, different damage scenarios were simulated by decreasing the beam stiffness by the minimum damage $k_{dam,i} = k_i(1 - \Delta_i)$, one at the time, and it was observed whether the test statistic reacted in the predicted manner. Therefore, the damaged state PDF was evaluated empirically in another Monte Carlo experiment with 100 data sets and $T = 1$ min. A correct prediction was characterized by an empirical damaged state PDF identical to the theoretical one or by a measured type II error β_{emp} identical to the theoretical one used for the prediction. In this paper, the power of the test was used to verify the predictions, *i.e.* the probability that a damaged structure is correctly classified as damaged.

$$Power = 1 - \beta_{emp} \stackrel{!}{=} 1 - \beta = 98\% \tag{19}$$

For visualization, representative results of the experiments were plotted in Fig. 4 and 5, where the empirical distributions of the test statistic were plotted in a blue histogram, together with the predicted damage state PDF (solid black line) and vertical dotted lines indicating the theoretical safety threshold. Please note that the figures only show the results from one single run, which are subject to uncertainties in both the reference and the test state. To quantify these uncertainties, the experiment was repeated 21 times, and the mean results are given in Table 1 and 2 including the standard deviations.

4.4.1. Parametric Damage Detection Test

The accuracy of the predictions could be validated visually in Fig. 5, as the empirical distributions in the damaged states followed the predicted ones. The similarity was confirmed by the values for the power of the test in Table 1, which ranged between 93.3% and 97.5% for Beam 1 - 6, so the maximum deviation from the target value of 98% was 4.7%. The mean power of the test averaged over all damage scenarios was 95.9%, and thus 2.1% below the target value. The inaccuracies could be tied back to a slight bias in the healthy state PDF, meaning the theoretical safety threshold value marginally overestimated the empirical 2% quantile of the empirical distribution. Nonetheless, it was deemed beneficial to use the theoretical safety threshold because it allowed for the time-consuming part of the training state (the empirical evaluation) to be skipped. In other words, there appeared to be a trade-off between increasing the accuracy of the predictions and maximizing the numerical efficiency of the estimation procedure.

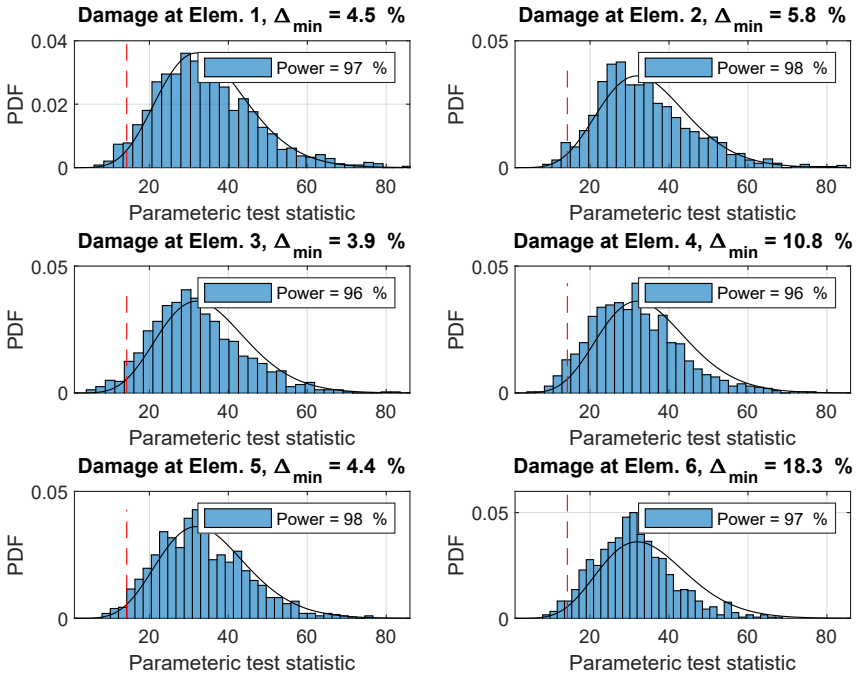


Figure 4: Validating the minimum detectable damage for the parametric test.

Table 1: Empirical power of the test for both damage detection tests, averaged over 21 runs.

No.	Detection test	Power of the test μ/σ [%]						
		Beam 1	Beam 2	Beam 3	Beam 4	Beam 5	Beam 6	Averaged
1	Parametric	96.7/1.8	97.5/1.6	96.4/1.8	95.2/2.6	96.3/2.3	93.3/4.4	95.9/2.4
2	Non-parametric	95.7/2.4	96.9/2.4	93.4 /3.5	92.5/3.1	93.5/2.7	96.4/3.0	94.7/2.8

The minimum detectable damage ranged between 4.0% and 18%, which was very low considering the short measurement duration of 1 min. Interestingly, a large Fisher information did not inevitably correspond to a high damage sensitivity, because the predictive formula also takes into account the parameter's magnitude $\theta_{0,i}$. For example, the main diagonal value of the Fisher information of Parameter 2 was greater than for Parameter 1, see Fig. 3. However, the beam stiffness of Beam 1 was twice as high reducing the minimum damage in Beam 1 to 4.55%, and thus, below 5.83% in Beam 2.

4.4.2. Non-Parametric Damage Detection Test

The accuracy of the predictions could be validated for the non-parametric test as well, see Figure 5, and the values for the power of the test ranges between 92.5% and 96.9%, with a maximum deviation of 5.5% and an averaged deviation of 2.3% from the target value of 98%, see Table 1.

The inaccuracies in the prediction, in particular in comparison to the parametric detection test, were most likely due to the additional bias that is introduced through the empirical curve-fitting. Notwithstanding, the results showcased that the empirical curve-fitting was a suitable approach to roughly estimate the number of degrees of freedom k of the chi-square distribution, so it was a helpful empirical means to fill the theoretical gap. Another contribution was the verification that the Fisher information from the parametric test could indeed be used for the non-parametric test. Since the number of DOFs of the healthy state PDF was greater for the non-parametric test, the distribution was wider, and a greater non-centrality was necessary (greater damage), so the damaged distribution could be discriminated from the healthy one. In other words, the non-parametric test was less sensitive to small damages than the parametric detection test. A great advantage of the non-parametric test was, however, that no parametrization was required for the damage diagnosis, so it could be appropriate for monitoring applications where no accurate finite element model is available.

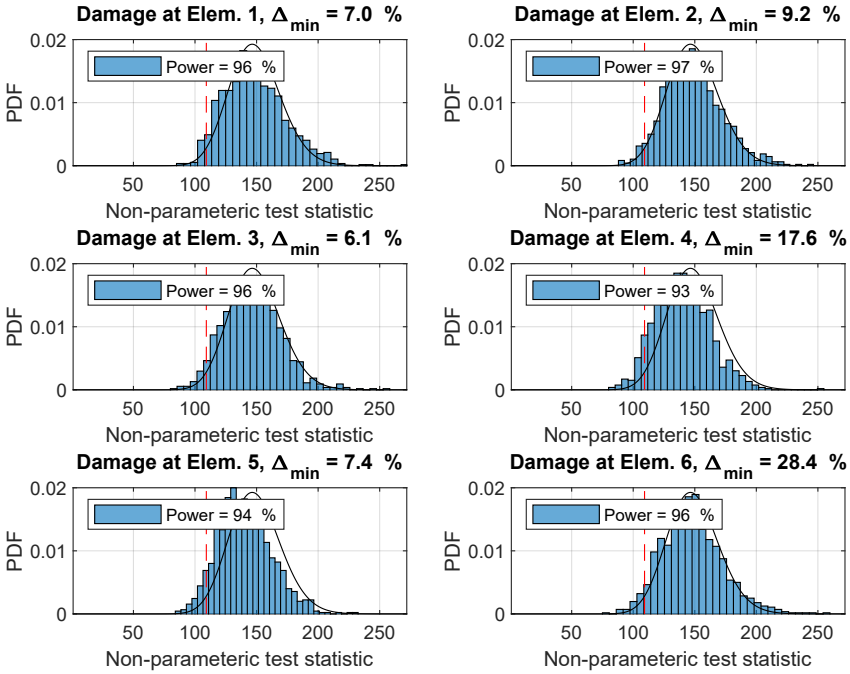


Figure 5: Validating the minimum detectable damage for the non-parametric test.

Table 2: Minimum detectable damage for both damage detectiont tests, averaged over 21 runs.

No.	Detection test	Minimum detectable damage μ/σ (%)					
		Beam 1	Beam 2	Beam 3	Beam 4	Beam 5	Beam 6
1	Parametric	4.55/0.12	5.83/0.15	4.02/0.1	11.03/0.45	4.49/0.20	17.94/0.84
2	Non-parametric	7.13/0.73	9.07/0.26	6.23/0.19	17.02/0.42	6.98/0.24	27.79/0.78

4.5. Discussion

The presented example, although simple, showcased the accuracy of the predictive formula for both the parametric and non-parametric damage detection test. One of the basic assumptions was a full rank sensitivity matrix, an assumption that is fulfilled for a 6-DOF mass-and-spring system. Before closing this paper, the findings for the monitoring problem at hand are generalized for varying design parameters. The following list of remarks also aids in understanding the physical meaning of the predictive formula in Eq. (17) from a theoretical standpoint.

- *Remark 1*: The larger the sample size N, the higher the damage sensitivity of the subspace-based damage detection tests, in an asymptotic manner. The sample size could be increased by extending the measurement duration T or tuning the sampling frequency f_s.
- *Remark 2*: In the presented example, it appeared that increasing the magnitude of the reference parameter $\theta_{0,i}$ leads to a decreasing (relative) minimum detectable damage Δ_i, despite the fact that $\theta_{0,i}$ also influences the Fisher information. That means, for example, that smaller damage percentages can be detected in stiff elements.
- *Remark 3*: The stricter the requirements regarding the reliability of the test, defined through the non-centrality parameter λ, the smaller the sensitivity of the damage diagnosis toward small damages.
- *Remark 4*: The parameters to be monitored remain user-defined, and it is possible to monitor changes in the mass, stiffness and/or damping properties.

The central element of this paper was the Fisher information matrix. It was used as a measure for the detectability of damage and linked the non-centrality in the statistical test to structural changes in a corresponding finite element model. However, it appeared that the minimum detectable damage also depended on the magnitude of the structural parameter to be monitored, see $\theta_{0,i}$ in Eq. (17). In this sense, a more suitable measure for the detectability of damage could be obtained by rearranging the predictive formula, for example, for the minimum measurement duration.

$$T = \frac{\lambda}{f_s \Delta_i^2} \left(\frac{1}{\theta_{0,i}^2 \cdot F_{ii}} \right) [s] \tag{20}$$

5. CONCLUSIONS

In this paper, a formula was developed that allows for the prediction of the minimum detectable damage for subspace-based damage diagnosis. By applying it to a simple mass-and-spring system, it was possible to illustrate both the effectiveness and accuracy of the predictions. A notable theoretical contribution was the extension of the theory to the non-parametric test, where theoretical concepts are mixed with auxiliary empirical means to determine the healthy state. Moreover, a code-based reliability concept was introduced that can be used to fix the non-centrality parameter based on user-defined requirements. Ultimately, the minimum measurement duration was proposed as a measure for the detectability of damage.

A major limitation is that the predictive formula only holds true for full rank sensitivitiy matrices, a condition that may be violated for any structure where different structural parameters cause a similar deviation in the Gaussian residual. This matter will be the subject of future studies.

ACKNOWLEDGMENTS

The financial support from the German Academic Exchange Service (DAAD) and the Natural Sciences and Engineering Research Council of Canada (NSERC) is gratefully acknowledged.

REFERENCES

[1] Farrar, C., & Worden, K. (2012). *Structural health monitoring: A machine learning perspective*. Oxford, U.K.: Wiley.

[2] Schnellenbach-Held, M., Karczewski, B., & Kühn, O. (2014). *Intelligente Brücke - Machbarkeitsstudie für ein System zur Informationsbereitstellung und ganzheitlichen Bewertung in Echtzeit für Brückenbauwerke*. Berichte der Bundesanstalt für Strassenwesen Brücken- und Ingenieurbau. Bremen, Germany: Fachverlag NW.

[3] Benveniste, A., Basseville, M., & Moustakides, G. (1987). The asymptotic local approach to change detection and model validation. *IEEE Transactions on Automatic Control*, *32*(7), 583–592.

[4] Basseville, M., Abdelghani, M., & Benveniste, A. (2000). Subspace-based fault detection algorithms for vibration monitoring. *Automatica*, *36*(1), 101–109.

[5] Balmès, É., Basseville, M., Mevel, L., Nasser, H., & Zhou, W. (2008). Statistical model-based damage localization: a combined subspace-based and substructuring approach. *Structural Control and Health Monitoring*, *15*(6), 857–875.

[6] Döhler, M., Mevel, L., & Hille, F. (2014). Subspace-based damage detection under changes in the ambient excitation statistics. *Mechanical Systems and Signal Processing*, *45*(1), 207–224.

[7] Döhler, M., Mevel, L., & Zhang, Q. (2016). Fault detection, isolation and quantification from Gaussian residuals with application to structural damage diagnosis. *Annual Reviews in Control*, *42*, 244–256.

[8] Döhler, M., Kwan, K., & Bernal, D. (2013). Optimal sensor placement with a statistical criterion for subspace-based damage detection. In *Proceedings of the IMAC - 31st International Modal Analysis Conference* (Vol. 4, pp. 219–229). New York: Springer.

[9] Basseville, M., Mevel, L., & Goursat, M. (2004). Statistical model-based damage detection and localization: subspace-based residuals and damage-to-noise sensitivity ratios. *Journal of Sound and Vibration*, *275*(3-5), 769–794.

[10] Heylen, W., & Sas, P. (1997). *Modal analysis theory and testing*. Belgium: K. U. Leuven.

[11] Allahdadian, S. (2017). *Robust statistical subspace-based damage assessment* (Doctoral dissertation, University of British Columbia, Vancouver).

[12] Wenzel, H. (2009). *Health monitoring of bridges*. Chichester U.K.: Wiley.